Flow and transport in tissue engineering scaffolds: a network modelling approach

*Steven R. McDOUGALL [1], Sarah L. WATERS [2]

1: Institute of Petroleum Engineering, Heriot-Watt University, UK
Tel.: ++44 (0)131 451 3166; Fax: ++44 (0)131 451 3127
Email: steve.mcdougall@pet.hw.ac.uk
* Corresponding author

2: Oxford Centre for Industrial and Applied Mathematics, Oxford University, UK
Tel.: ++44 (0)1865 280 141; Fax: ++44 (0)1865 270 515
Email: waters@maths.ox.ac.uk

Abstract Tissue engineers aim to grow functional tissues in the laboratory. One approach is to seed cells on a porous biomaterial scaffold, which is then cultured in a flow perfusion bioreactor. Such bioreactors enhance the transport of nutrients and growth factors to the cells by convection, and provide mechanical loads to mechanosensitive tissues. In this paper, we adopt a network modelling approach to provide insight into the nature of the flow, nutrient transport and cell distribution through the porous scaffold. The approach resolves flow and nutrient transport at the pore scale, and thus enables the local cellular environment to be determined. We demonstrate how this method can be used to study the impact of scaffold geometry (*e.g.* porosity, connectivity) on the cellular environment, and hence provide insight into the optimum culture conditions required to obtain functional tissues.

Keywords: Tissue engineering, Network modelling, Porous flow, Transport

1. Introduction

Tissue engineers aim to grow functional tissues and organs in the laboratory to replace those that have become defective through age, trauma and disease, and which can be used in drug screening applications. To engineer tissues with the desired compositional, biomechanical and biochemical properties (in the sense that they mimic the *in vivo* tissue), accurate control of both the biomechanical and biochemical environment of the growing tissue construct is essential.

One approach is to seed cells on a porous biomaterial scaffold, which is then cultured in a flow perfusion bioreactor (in which culture medium is driven through the scaffold under an imposed pressure gradient or flux). The composition of the culture medium may be altered by the addition of key nutrients and growth factors required by the cells being cultured. In static culture, the key transport mechanism by which these nutrients and growth factors reach the cells is diffusion, which necessarily limits the tissue size. Dynamic culture within a flow perfusion bioreactor enables transport to the cells to be enhanced by convection, and additionally the flow assists in the removal of associated degradation products. Furthermore, flow perfusion bioreactors are increasingly being used to provide mechanical loads to mechano-sensitive tissues, *e.g.* many studies have shown that stimulation via fluid shear stress enhances bone tissue formation (see, *e.g.*, You *et al.* 2001).

A variety of dynamic flow-perfusion bioreactors have been developed. These include spinner-flasks, rotating-wall vessels, hollow-fibre bioreactors and direct perfusion bioreactors (see Martin, Wendt and Heberer 2004 and references therein). A range of techniques for biomaterial scaffold fabrication exist, which enable scaffold porosity, pore interconnectivity, scaffold surface chemistry (and hence wettability etc) to be controlled (Hutmacher 2000). Thus there is a wealth of different choices available for bioreactor design and porous biomaterial scaffold. Attention is now focused on the development

of 'application-driven' bioreactors, which attempt to recreate an environment that is appropriate to the tissue under consideration. To achieve this, it is essential that tissue engineers are able to quantify the underlying flow and transport properties of the bioreactor system. Mathematical modelling is a technique that can be used to provide quantitative insights into these bioreactor properties.

Examination of any thin section taken from a porous biomaterial scaffold immediately demonstrates why the modelling of fluid flow and nutrient transport through these structures is such a challenging task. Underlying network topologies are complex, consisting of tortuous interconnected channels separated from one another by polymer struts of varying thickness (see Mather et al. (2009)). Similar modelling issues are encountered in the contexts of petroleum engineering and hydrology, where the main focus of investigation is the prediction of multiphase flow properties associated with rocks and soil. In this paper, network modelling techniques widely used in the petroleum industry are adapted to the study of flow within tissue constructs.

A fully interconnected network model was first developed by Fatt (1956) for investigating the flow of oil and water through reservoir rock and, although the two-dimensional lattice used was extremely small (200 - 400 elements), the novelty of the approach encouraged great interest in the subject. A substantial literature relating to pore-scale modelling now exists and the technique has developed to such an extent that it is now possible to reconstruct complex rocks via 3D imaging (x-ray micro-CT) followed by numerical network extraction (Oren et al.1997; Sok et al. 2002). Moreover, increasing computer power has recently enabled pore-scale models up to 1m in length to be constructed for use in laboratory-scale gas migration and viscous fingering studies (Bondino et al. 2005, 2007, 2009).

There are several examples of network modelling approaches being applied to biologically-relevant systems, *e.g.* blood flow within capillary beds. In McDougall et al. (2002), flow through vascular networks was considered to examine the efficiency of chemotherapy treatments as they passed from a nearby parent vessel to a distal tumour surface. Vascular architectures obtained from hybrid discrete/continuous models of endothelial cell migration were simply mapped onto templates of interconnected capillary elements and flow calculations performed. Stéphanou et al. (2005a) extended this work by considering how the removal of certain capillaries affected the distribution of blood flow in the system ─ capillary pruning algorithms were designed to reflect how different anti-vascular and anti-angiogenic drugs were thought to operate *in vivo* and simulations were carried out using fully 3-dimensional networks. Stéphanou et al., (2005b) refined the model further by considering how adaptive vessel remodelling affected the supply of oxygen and drugs to tumour cells. This refinement included variable blood viscosity and evolving capillary vessels that dilated or constricted both spatially and temporally in response to a variety of cellular and metabolic cues. Precise details of this approach to flow modelling are available in McDougall et al. (2006) and are briefly summarised in Section 2.

In this paper, we illustrate how such a network modelling approach can be used to provide insight into the nature of the flow, nutrient transport and cell distribution through a porous biomaterial scaffold which has been seeded with cells and placed within a perfusion bioreactor. The approach resolves flow and transport at the pore scale, and thus enables the local cellular environment to be determined, *e.g.* local wall shear stress and nutrient concentration. We demonstrate how this method can be used to study the impact of varying bioreactor operating conditions (*e.g.* flow rate) and scaffold geometry (*e.g.* porosity, connectivity) on the cellular environment, and hence improve understanding of the optimum culture conditions required to obtain functional tissues. Particular goals are to produce homogeneous tissue constructs, and to prevent washout of cells from the porous biomaterial scaffold.

2. Modelling Background

2.1 Bioreactor-scaffold system

To illustrate the effectiveness of our approach, we consider a simplified bioreactor-scaffold system. The scaffold is represented as either a 2D lattice or 3D cubic network of interconnected pores. Flow of a viscous, incompressible fluid (representing the culture medium) is driven through this system at a prescribed flow rate imposed at the upstream scaffold face. Additionally, nutrient at constant concentration is injected at the upstream face continuously. The scaffold is seeded with cells, which, for the purpose of this study, are assumed not to affect the fluid flow and to be biologically inert, i.e. they do not proliferate or differentiate.

Note that the network modelling approach described here is extremely versatile and many simplifying assumptions may be relaxed. For example, the cells may be allowed to proliferate in response to elevated levels of wall shear stress.

2.2 Network modelling & wall shear stress

In its most general form, the flow model developed here consists of a three-dimensional cubic network of *bond elements (pores)*. These bonds can be thought of as straight cylindrical capillary elements, although the constraint of cylindrical geometry can easily be relaxed without loss of generality, so long as a local linear relationship between pressure drop and flow-rate can be established. The bond elements meet at *nodes*. For porous media studies, pressures are specified at the inlet and outlet faces of the system and each capillary element is randomly assigned a radius drawn from an input probability distribution function (PDF). For most of the simulations described here, a uniform PDF has been assumed (although this assumption will be relaxed later when considering experimental samples). It should be noted that the experiments motivating this study generally employ a constant flow-rate condition and so inlet and outlet pressures cannot simply be stipulated *a priori* ─ the corresponding pressure gradient must be adjusted *a posteriori* by means of a numerical simulation that honours both the imposed flow constraint and case-specific scaffold permeability.

For a single capillary element of radius R and length L, the elemental fluid flow rate in the capillary is assumed to be given by Poiseuille's law:

$$Q = \frac{\pi R^4 \Delta P}{8 \mu L} \qquad (1)$$

where μ is the fluid viscosity and ΔP the pressure drop across the element. To determine the flow distribution throughout a network of interconnected capillary elements having distributed radii, conservation of fluid flow is applied at each junction where capillary elements meet. Suppose $Q_{(i,j)}$ is used to denote the flow into node i from node j. Hence, for each node i the following expression can be written:

$$\sum_{k=1}^{k=N} Q_{(i,k)} = 0 \qquad (2)$$

where the index k refers to adjacent nodes and N=4 in a fully connected regular 2D grid or 6 in 3D. This procedure leads to a set of linear equations for the nodal pressures which can be solved numerically using any of a number of different algorithms. Once nodal pressures are known, equation (1) can be used to calculate the flow in each capillary element in turn. See McDougall and Sorbie (1997) for further details.

Assuming cylindrical bond elements, the wall shear stress can be calculated using the expression:

$$\tau_w = \frac{4\mu}{\pi R^3} |Q| \qquad (3)$$

where |Q| is the absolute value of the flow in the bond element under consideration and other parameters are as described earlier. The fact that the bond elements are connected in a network means that the spatial distribution of wall shear stress cannot simply be predicted analytically: numerical simulation is required.

2.3 Nutrient transport

To model the time evolution of nutrient transport through the tissue scaffold, a simple nodal mixing algorithm is adopted that enables concentration profiles of an injected nutrient to be tracked as follows. Having solved for the nodal pressures and elemental flows throughout the system, as described in Section 2.1, a nutrient at concentration C_{max} is injected continuously across the entire upstream face of the network. Over a given time-step, the following procedure is adopted:
(i) the total mass of nutrient flowing into each node from neighbouring bond elements is calculated;
(ii) perfect mixing is intrinsically assumed at each node and nutrient concentrations in all outflow bonds are updated after flow-weighted partitioning of the available nutrient mass at the node.

Caution has to be exercised to ensure that mass conservation is satisfied at all times. The (varying) time-step chosen during the simulation is consequently calculated from:

$$\Delta t = MIN\left\{\frac{\pi r_i^2 L_i}{Q_i}\right\} \qquad (4)$$

where the subscript *i* is used here to denote a bond element.

2.4 Cell washout

Although our methodology may be developed to consider coupling between the local biomechanochemical environment and the cellular response, we restrict attention here to the issue of cell washout, whereby individual cells are convected from their original seeding location downstream towards the outlet scaffold face. Cells are initially placed at the centre of randomly-determined elements within the network and the scaffold is perfused with fluid. No cell-cell or cell-substrate adhesion is included here ─ the cells are simply free to explore the tortuous pathways until they either leave the system or became effectively trapped in elements characterised by low shear. Computationally, all cell positions within individual elements must be recalculated whenever a cell reaches a junction. The destination element for the new arrival is based upon flow-weighted probabilities corresponding to each outflowing element ─ the cell is convected into its new host element and the positions of all other cells in the system are updated. This process is repeated until the total convection time reaches the time-step defined in (4). Note that there is no restriction on the number of cells that can be present in an element at any given time.

3 Input data for 2D flow simulations

The choice of parameter values used in the numerical simulations is motivated by biomaterial scaffold data given in Mather et al. (2009). These scaffolds are fabricated by depressurising a polymer powder saturated with supercritical CO_2. This creates a foam which cools to give a vitrified porous scaffold, the properties of which can be varied by controlling the molecular weight of the powder and the CO_2 venting time. Two examples, $P_{DL}LA$ 15kDa (30 min venting time) and $P_{DL}LA$ 52kDa (60 min venting time) are considered.

We first simulate 2D networks, in order to help visualisation of the underlying scaffold structure and fluid dynamics. Pore size distribution data derived from μ x-ray CT images were reported in Mather et al. (2009), together with scaffold porosities and laboratory injection rate. However, since no data pertaining to pore length was available this is determined analytically as follows. Consider a cubic network of nodal dimensions n_x x n_y x n_z consisting of circular cylinders each of mean radius <R> and length L_p. The pore volume of the network is given by:

$$V_p = 3n_x n_y n_z \pi \langle R \rangle^2 L_p$$

and the bulk volume is given by:

$$V_B = n_x n_y n_z L_p^{\ 3}$$

Hence the porosity of the scaffold is given by $\phi = V_p/V_B$ which can be rearranged to give:

$$L_p = \sqrt{\frac{3\pi\langle R\rangle^2}{\phi}} \quad (5)$$

For the 6 samples reported in Mather et al. (2009), this gives a mean pore length of approximately 500μm and this value is used in the following 2D simulations.

Finally, although laboratory flow-rate was supplied in the paper, no pressure drop was measured across experimental samples and this is a vital input required by the network model simulation. To determine an average pressure gradient for use in the simulations, a 10mm x 10mm x 4mm 3D network was constructed using mean pore sizes and mean pore lengths derived from the experimental data. These sample dimensions were the same as those used in an earlier laboratory study by the same group. A laboratory flow-rate of 0.1ml/min ($1.67\text{x}10^{-9}$ m^3/s) was matched by adjusting the pressure drop across the 3D network, resulting in a calculated pressure gradient of 28.75Pa/m. This gradient was then applied across a 2D analogue, and a new 2D injection constraint was subsequently derived. This gave a 2D injection rate of $4.4\text{x}10^{-12}$ m^3/s.

For the 2D simulations that follow, a large (50mm x50mm), square scaffold was considered (comprising 100 x 100 nodes, which corresponds to approximately 20,000 pores).

4. 2D sensitivity studies

In the following simulations the notation U(a,b) denotes bond element radii distributed randomly from a uniform pore size distribution between a and b (in μm). The Z value indicates the average number of bond elements that meet at a junction. The base case corresponds to a=1μm, b=100μm, and Z=4.

4.1 Wall shear stress distribution

Figure 1 shows the distribution of wall shear stress. In Figure 1a, the connectivity of the network is varied**.** As the connectivity decreases the distribution 'flattens' and the relative number of bond elements having the lower values of shear stress decreases, reflecting the fact that there are fewer pathways for fluid flow, and, accordingly, the wall shear stress values are higher. Figure 1b illustrates the effect of pore size variance on the wall shear stress distribution (in all cases Z=4). As the variance decreases an interesting feature is the appearance of a 'bimodal' shear stress distribution. This feature becomes more marked as the variance decreases to zero, and reflects the fact that in a network of bond elements of equal radii, the flow will be in the axial direction (aligned with the direction of the pressure drop), with no transverse flow. Finally, Figure 1c shows the effect of increasing the mean bond element radii: the typical wall shear stress values subsequently decrease.

(a)

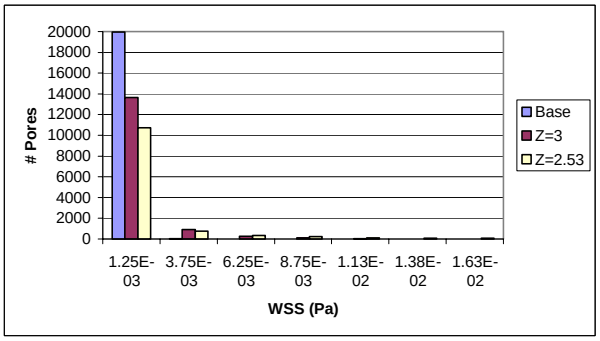

(b)

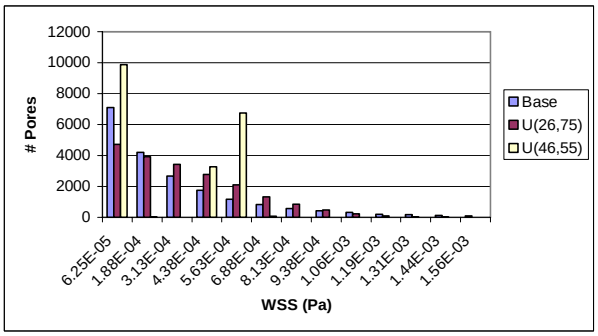

(c)

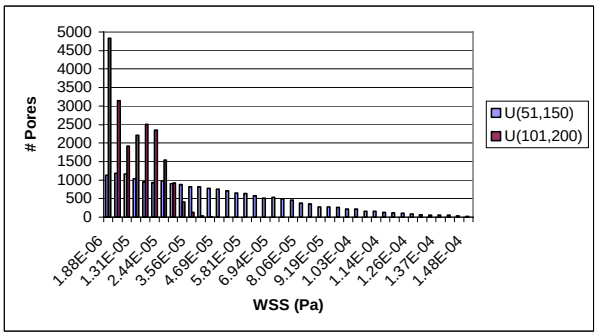

Figure 1. The influence of (a) connectivity, (b) bone element size variance and (c) mean bond element size on the wall shear stress distribution.

4.2 Nutrient transport

Figure 2 shows the total amount of nutrient that exits the network at the downstream face over time. Decreasing the connectivity results in less nutrient efflux, whilst decreasing the bond element radii variance results in efflux at earlier times (due to the predominance of the flow in the axial direction). Increasing the mean bond element radii increases the time to non-zero efflux, due to the reduction in fluid velocity within each element.

(a)

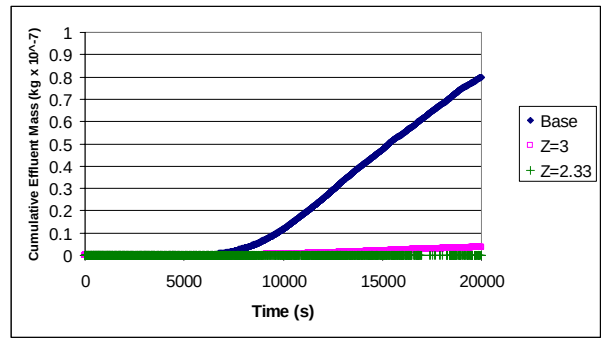

(b)

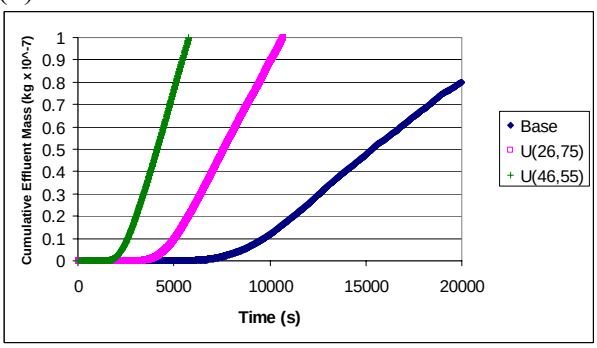

(c)

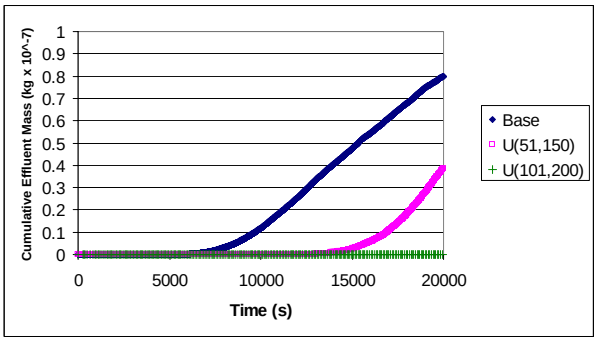

Figure 2. The influence of (a) connectivity, (b) bone element size variance and (c) mean bond element size on nutrient transport. Injected nutrient concentration = 1kg/m^3. Selected concentration profiles at time t=10^4 s are also presented for sensitivity (a).

4.3 Cell washout

Figure 3 illustrates the effects of connectivity, mean and variance of the bond element radii on cell washout. Wash out is clearly reduced as the connectivity decreases, the variance increases and the mean bond element radius increases.

(a)

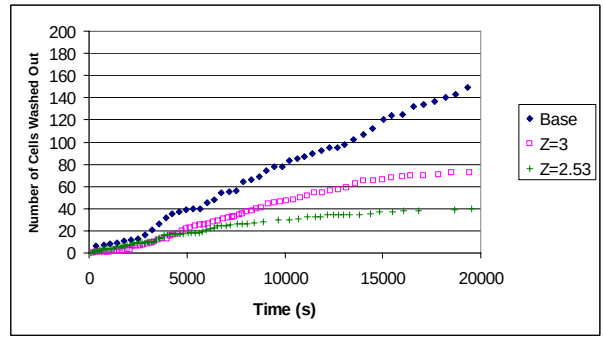

(b)

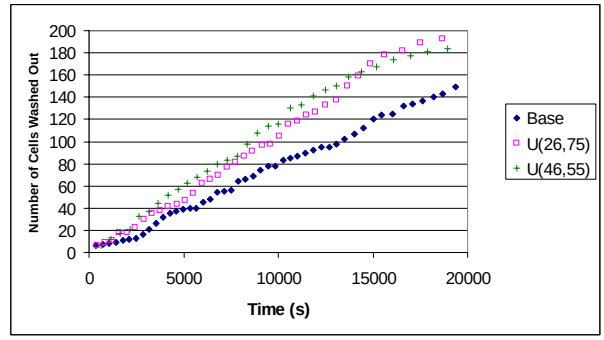

(c)

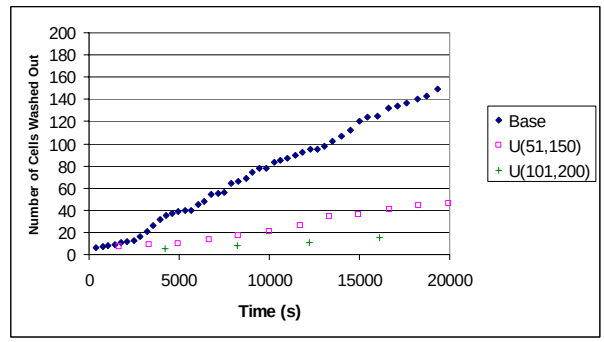

Figure 3. The influence of (a) connectivity, (b) bone element size variance and (c) mean bond element size on cell washout. Selected cell populations at time

$t=10^4$ s are also presented for sensitivity (a).

5. 3D simulations

We now make quantitative predictions of cell washout, nutrient transport and wall shear stress in the 3D scaffolds reported in Mather et al. (2009). Two scaffolds, $P_{DL}LA$ 15kDa (30 min venting time) and $P_{DL}LA$ 52kDa (60 min venting time) were selected from those presented, as these represent the extremes in terms of scaffold porosity (90% and 62%, respectively).

Pore size distributions were matched to experimental data and the corresponding histograms are shown in Figure 4. Average pore lengths of 420µm and 545µm were calculated from equation 5 and total network dimensions of 10mm x 10mm x 10mm were adopted in line with experimental samples. This gives networks containing 24 x 24 x 24 nodes ($P_{DL}LA$ 15kDa) and 18 x 18 x 18 nodes ($P_{DL}LA$ 52kDa). Both networks were assumed to be fully connected (Z=6 in 3D) and each was initially seeded with 800 cells.

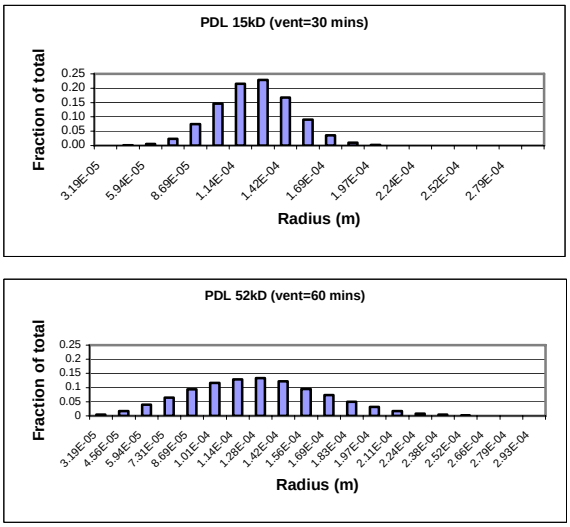

Figure 4. Pore size distributions for the two scaffolds under consideration.

As before, we can use this approach to quantify nutrient efflux and cell washout from the biomaterial scaffold. An interesting feature is that the bond element distribution with smaller variance (15kD) again exhibits the bimodal distribution of wall shear stress, from which it might be inferred that the resulting engineering construct will be heterogeneous.

6. Discussion

In this paper we have illustrated the effectiveness of a network modelling approach in providing insight into shear stress distribution, nutrient transport and cell washout. A key tissue engineering goal is to engineer constructs with homogeneous properties. One way to achieve this is to provide a homogeneous environment for the cells, both in terms of wall shear stress and nutrient concentration. Our results clearly indicate that to achieve a relatively uniform wall shear stress throughout the network the bond element radii should have a large variance. Another consideration is the desire to minimise cell washout, and nutrient efflux. Again, our results indicate that increasing the mean pore size radius and/or reducing pore connectivity can be advantageous in achieving these goals.

(a)

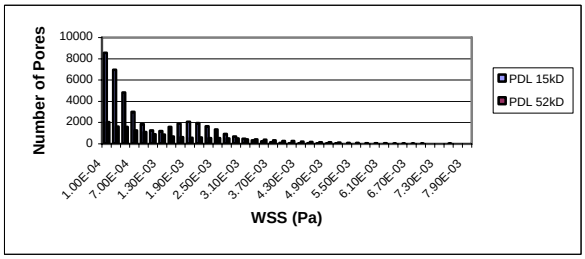

(b)

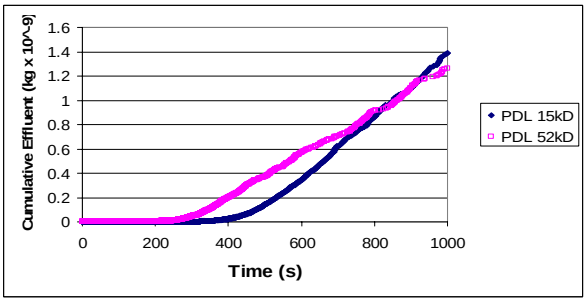

(c)

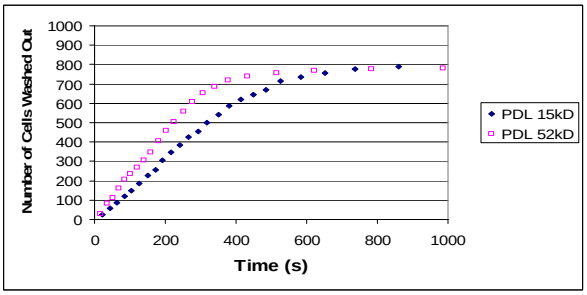

Figure 5. (a) Wall shear stress distributions, (b) cumulative effluent, and (c) degree of cell wash-out for the 3D simulations described in Section 5.

We stress that we have chosen a simplified system to illustrate the effectiveness of this approach. The approach, however, is sufficiently versatile that additional degrees of biological complexity can be added. For example, a key development will be the coupling between the cell biology and the biochemical and biomechanical environment: in regions where the environment is favourable to cell proliferation, blocking of bond elements is likely to occur, and the resulting spatial adaptations to wall shear stress and nutrient transport throughout the network will effect the subsequent evolution of the tissue construct.

In conclusion, theoretical studies of the type described here, coupled with carefully controlled experiments, have the potential to provide significant insights into tissue engineering protocols, and to enable the identification of optimum bioreactor and scaffolds properties to engineer constructs with the desired properties.

Acknowledgements
SLW would like to thank the EPSRC for funding in the form of an Advanced Research Fellowship.

Bondino, I, McDougall, S.R. and Hamon, G., 2005. Pore Network Modeling of Heavy Oil Depressurization: . SPE J. 10, 196-205.

Bondino, I., Long, J., McDougall, S.R. and Hamon, G., 2007. A pore scale network modelling study of gravitational effects during solution gas drive: results from macro-scale simulations. SPE 107556.

Bondino, I., McDougall, S.R. and Hamon, G., 2009. A pore-scale modeling approach to the interpretation of heavy oil pressure depletion experiments. J. Pet. Sci. Eng. 65, 14–22.

Fatt, I., 1956. The network model of porous media I. Capillary pressure characteristics. Pet. Trans. 207, 144-159.

Hutmacher, D.W., 2000. Scaffolds in tissue engineering bone and cartilage. Biomat. 21, 2529-2543.

Martin, I., Wendt, D. and Heberer, M., 2004. The role of bioreactors in tissue engineering. Trends Biotech. 22, 80-86.

Mather M.L., Brion M., White L.J., Shakesheff K.M., Howdle S.M., Morgan S.P. and Crowe J.A., 2009. Time-lapsed imaging for in-process evaluation of supercritical fluid processing of tissue engineering scaffolds. Biotech. Prog. Accepted 2009

McDougall, S.R. and Sorbie, K.S., 1997. The application of network modelling techniques to multiphase flow in porous media. Pet. Geos. 3, 161-169.

McDougall, S.R., Anderson, A.R.A, Chaplain, M.A.J and Sherratt, J.A. 2002. Mathematical Modelling of Flow Through Vascular Networks: Implications for Tumour-Induced Angiogenesis and Chemotherapy Strategies. Bull. Math. Biol. 64, 673-702.

McDougall, S.R., Anderson, A.R.A and Chaplain, M.A.J. 2006. Mathematical Modelling of Dynamic Adaptive Tumour-Induced Angiogenesis: Clinical Implications and Therapeutic Targeting Strategies. J. Theor. Biol. 241, 564-589.

Øren, P.-E., Bakke, S. and Arntzen, O.J. 1997 Extending predictive capabilities to network models. SPE 38880.

Sok, R.M., Knackstedt, M.A., Sheppard, P., Pinczewski, W.V., Lindquist, W.B., Venkatarangan, A. and Paterson, L., 2002. Direct and stochastic generation of network models from tomographic images; effect of topology on residual saturations. Trans. Porous Media. 46, 345-372.

Stephanou, A, McDougall, S.R., Anderson, A.R.A. and Chaplain, M.A.J. ,2005. Mathematical Modelling of Flow in 2D and 3D Vascular Networks. Math. Comp. Mod. 41, 1137-1156.

Stephanou, A, McDougall, S.R., Anderson, A.R.A. and Chaplain, M.A.J. , 2006. Dynamic Modelling of Tumour-Induced Angiogenesis. Math. Comp. Mod., 44, 96-123.

You, L., Cowin, S.C., Schaffler, M.B. and Weinbaum, S. , 2001. A model for strain amplification in the actin cytoskeleton of osteocytes due to fluid drag on pericellular matrix. J. Biomech. 34, 1375-86.